# UNIVERSITY<sup>OF</sup> BIRMINGHAM University of Birmingham Research at Birmingham

# Impact of air emissions from shipping on marine phytoplankton growth

Zhang, Chao; Shi, Zongbo; Zhao, Junri; Zhang, Yan; Yu, Yang; Mu, Yingchun; Yao, Xiaohong; Feng, Limin; Zhang, Fan; Chen, Yingjun; Liu, Xiaohuan; Shi, Jinhui; Gao, Huiwang

DOI: 10.1016/j.scitotenv.2021.145488

License: Creative Commons: Attribution-NonCommercial-NoDerivs (CC BY-NC-ND)

Document Version Peer reviewed version

#### Citation for published version (Harvard):

Zhang, C, Shi, Z, Zhao, J, Zhang, Y, Yu, Y, Mu, Y, Yao, X, Feng, L, Zhang, F, Chen, Y, Liu, X, Shi, J & Gao, H 2021, 'Impact of air emissions from shipping on marine phytoplankton growth', *Science of the Total Environment*, vol. 769, 145488. https://doi.org/10.1016/j.scitotenv.2021.145488

Link to publication on Research at Birmingham portal

#### **General rights**

Unless a licence is specified above, all rights (including copyright and moral rights) in this document are retained by the authors and/or the copyright holders. The express permission of the copyright holder must be obtained for any use of this material other than for purposes permitted by law.

•Users may freely distribute the URL that is used to identify this publication.

•Users may download and/or print one copy of the publication from the University of Birmingham research portal for the purpose of private study or non-commercial research.

•User may use extracts from the document in line with the concept of 'fair dealing' under the Copyright, Designs and Patents Act 1988 (?) •Users may not further distribute the material nor use it for the purposes of commercial gain.

Where a licence is displayed above, please note the terms and conditions of the licence govern your use of this document.

When citing, please reference the published version.

#### Take down policy

While the University of Birmingham exercises care and attention in making items available there are rare occasions when an item has been uploaded in error or has been deemed to be commercially or otherwise sensitive.

If you believe that this is the case for this document, please contact UBIRA@lists.bham.ac.uk providing details and we will remove access to the work immediately and investigate.

# 1 Impact of air emissions from shipping on marine phytoplankton

- 2 growth
- 3
- Chao Zhang<sup>1, 2</sup>, Zongbo Shi<sup>3</sup>, Junri Zhao<sup>4</sup>, Yan Zhang<sup>4</sup>\*, Yang Yu<sup>1</sup>, Yingchun, Mu<sup>5</sup>, Xiaohong Yao<sup>1, 2</sup>,
  Limin Feng<sup>6</sup>, Fan Zhang<sup>7</sup>, Yingjun Chen<sup>4</sup>, Xiaohuan Liu<sup>1, 2</sup>, Jinhui Shi<sup>1, 2</sup> and Huiwang Gao<sup>1, 2</sup>\*
- <sup>1</sup> Key Laboratory of Marine Environment and Ecology, Ministry of Education of China, and Frontiers Science Center for
   Deep Ocean Multispheres and Earth System, Ocean University of China, Qingdao 266100, China
- <sup>2</sup> Laboratory for Marine Ecology and Environmental Sciences, Pilot National Laboratory for Marine Science and Technology,
   Qingdao 266071, China
- <sup>3</sup> School of Geography, Earth and Environmental Sciences, University of Birmingham, Birmingham B152TT, UK
- <sup>4</sup> Shanghai Key Laboratory of Atmospheric Particle Pollution and Prevention (LAP3), Department of Environmental Science
- 12 and Engineering, Fudan University, Shanghai 200092, China
- <sup>5</sup> Estuarine and Coastal Environment Research Center, Chinese Research Academy of Environmental Sciences, Beijing
   100012, China
- <sup>6</sup> State Key Laboratory of Atmospheric Boundary Layer Physics and Atmospheric Chemistry (LAPC), Institute of Atmospheric Physics (IAP), Chinese Academy of Sciences (CAS), Beijing 100029, China
- <sup>7</sup> Key Lab of Geographic Information Science of the Ministry of Education, School of Geographic Sciences, East China
   Normal University, Shanghai 200241, China
- 19

20 Corresponding author: Huiwang Gao (<u>hwgao@ouc.edu.cn</u>); Yan Zhang (<u>yan\_zhang@fudan.edu.cn</u>)

# 21 Abstract

With the rapid expansion of maritime traffic, increases in air emissions from shipping have exacerbated 22 numerous environmental issues, including air pollution and climate change. However, the effects of 23 such emissions on marine biogeochemistry remain poorly understood. Here, we collected ship-emitted 24 25 particles (SEPs) from the stack of a heavy-oil-powered vessel using an onboard emission test system and investigated the impact of SEPs on phytoplankton growth over the northwest Pacific Ocean 26 (NWPO). In SEP microcosm experiments conducted in oceanic zones with different trophic statuses, the 27 phytoplankton response, as indicated by chlorophyll a (Chl a), has been shown to increase with the 28 proportion of SEP-derived nitrogen (N) relative to N stocks (P<sub>SN</sub>) in baseline seawater, suggesting that 29 SEPs generally promote phytoplankton growth via N fertilisation. Simulations using an air quality 30 model combined with a ship emission inventory further showed that oxidised N (NO<sub>x</sub>) emissions from 31 shipping contributed ~43% of the atmospheric N deposition flux in the NWPO. Air emissions from 32 shipping (e.g. NO<sub>x</sub> and sulphur dioxide) also indirectly enhanced the deposition of reduced N that 33 existed in the atmosphere, constituting ~15% of the atmospheric N deposition flux. These results 34 suggest that the impact of airborne ship emissions on atmospheric N deposition is comparable to that of 35 land-based emissions in the NWPO. Based on the ship-induced P<sub>SN</sub> in surface seawater calculated by 36 modeling results and World Ocean Atlas 2013 nutrient dataset, and the well-established quantitative 37 relationship between Chl a and P<sub>SN</sub> obtained from microcosm experiments, we found a noticeable 38 change in surface Chl a concentrations due to N deposition derived from marine traffic in the NWPO, 39 particularly in the coastal waters of the Yellow Sea and open oceans. This work attempts to establish a 40 41 direct link between marine productivity and air emissions from shipping.

#### 42 **1. Introduction**

43 The rapid expansion of marine trade and rapid globalisation have increased the number of ships in recent years (Bencs et al., 44 2017). Such changes have led to continuous increases in the emissions of oxidised nitrogen (NO<sub>x</sub>), sulphur dioxide (SO<sub>2</sub>), 45 oxocarbons (CO<sub>2</sub> and CO), volatile organic compounds (VOCs), black carbon, trace metals and particulate matter (PM), 46 among others (Eyring et al., 2010). Considerable increases in PM and gaseous pollutants over frequently navigated waters have been observed in many studies (Eyring et al., 2010; Fan et al., 2016; Bencs et al., 2017). Such increases can alter the 47 48 microphysical properties of aerosols and clouds and affect radiative forcing, ultimately influencing climate (IPCC, 2007). 49 Ship emissions can also increase the bioavailability of nutrients such as iron (Fe) and nitrogen (N) in atmospheric deposition and potentially affect ocean biogeochemical processes (Boyd et al., 2007; Ito and Shi, 2016; Jickells et al., 2005 and 2017). 50 In general, the Fe solubility of mineral aerosols is as low as <1%, whereas that of particles emitted by the combustion of fuel 51 52 can be up to 77-81% (Schroth et al., 2009). Model results have predicted that air emissions from shipping in 2100 will contribute 30-60% of the soluble iron deposition over the high-latitude North Pacific and North Atlantic (Ito, 2013). 53 Anthropogenic emissions contribute >80% of the bioavailable N deposition to the ocean (Duce et al., 2008). More 54 55 specifically, ship emissions contribute  $\sim 15\%$  of anthropogenic NO<sub>x</sub> globally and are becoming increasingly important in 56 coastal areas (Corbett et al., 1999; Eyring et al., 2010; Chen et al., 2017a). The high-temperature combustion of fuel creates a 57 suitable environment for the formation of  $NO_x$  and increases the solubility of Fe and other nutrients (Turner et al., 2017). Thus, the use of fuel to sustain intensifying levels of marine traffic for the foreseeable future will increase the importance of 58 59 ships in anthropogenic emissions.

60

61 In practice, it is difficult to determine the impact of the deposition of air emissions from shipping on marine ecosystems 62 through direct field observations. One chief reason for this is that we cannot distinguish the impact of airborne ship

63	emissions from the impacts of other factors, such as water discharges from shipping and air emissions from continents
64	(Jagerbrand et al., 2019). Accordingly, most previous studies have evaluated the impact of air emissions from shipping on the
65	ocean using modeling approaches (Hunter et al., 2011; Hassellov et al. 2013; Raudsepp et al., 2019; Djambazov and
66	Pericleous, 2015; Zhang J. et al., 2019). For instance, chemical modeling has shown that ship-derived emissions of NO <sub>x</sub> and
67	SO <sub>2</sub> have only a small impact on the acidification of coastal waters (i.e. in the North Sea, Baltic Sea, and South China Sea
68	(SCS)) but could reduce the uptake of anthropogenic $CO_2$ in these areas (Hunter et al., 2011). Meanwhile, Hassellov et al.
69	(2013) argued that regional pH reductions in heavily trafficked waters were of the same order of magnitude as those induced
70	by CO2-driven acidification. More recently, Raudsepp et al. (2019) used a coupled biochemical and physical model to
71	simulate the impact of air emissions from shipping and found that ship-borne N deposition stimulated phytoplankton growth
72	(e.g. diatoms, flagellates) and decreased the phosphorus (P) stock in the surface seawater of the Baltic Sea. However, their
73	results showed that such changes induced by ship emissions had only a minor effect on the overall ecosystem. Hence, it is
74	necessary to obtain experimental evidence to accurately assess the impact of air emissions from shipping on the marine
75	environment and associated ecosystem.
76	

77 It is well known that N stocks are generally deficient relative to P stocks in most oceanic zones (Duce et al., 2008; Moore et 78 al., 2013; Kim et al., 2014). However, it is difficult to establish a quantitative relationship between atmospheric N input and 79 phytoplankton response. This is because N limitation in oceanic regions characterised by varying trophic statuses can lead to 80 different phytoplankton responses. For instance, the N input in mesotrophic to eutrophic seawater generally exerts a more 81 pronounced stimulation effect on large phytoplankton (cell size >2  $\mu$ m) than that in oligotrophic seawaters (Guo et al., 2012; Li et al., 2015). Moreover, studies have increasingly detected the prevailing co-limitation of phytoplankton (i.e. limitation by 82 83 two or more nutrients) across extensive areas of the upper oceans, especially in oligotrophic regions where nutrients are almost depleted (Moore et al., 2013; Li et al., 2015; Browning et al., 2017a; Zhang C. et al., 2018). Considering the 84

85	occurrence of nutrient co-limitation, the phytoplankton response to air emissions from shipping may be affected by several
86	factors rather than N alone (Chien et al., 2016; Zhang C. et al., 2018; Raudsepp et al., 2019). In addition, air emissions from
87	shipping (a typical combustion source) typically exhibit higher trace metal solubility than mineral dust (Ito, 2013; Turner et
88	al., 2017), which can increase the role of trace metals in affecting phytoplankton growth (Saito et al., 2008; Browning et al.,
89	2017b). Overall, variations in the trophic statuses and phytoplankton requirements of seawater increase the difficulty in
90	interpreting the mechanism of ship emissions in affecting marine primary production.

In recent years, the northwest Pacific Ocean (NWPO) has experienced some of the most rapid increases in shipping traffic 92 93 globally (Liu et al., 2016; Zhang et al., 2017; UNCTAD, 2019). In this region, enhanced shipping traffic has markedly 94 influenced the atmospheric composition and atmospheric deposition (Yau et al., 2012; Ito et al., 2013; Chen et al., 2017a, b). However, its effects on the marine ecosystem of the region remain unknown. To address this gap in knowledge, the present 95 96 study represents the first attempt to estimate the impact of ship-induced N deposition on primary production by combining 97 experimental, observational, and modeling measures. The study region included coastal seas and open oceans of the NWPO: 98 the SCS, Yellow Sea (YS), Kuroshio Extension (KE), and Kuroshio-Oyashio transition region (TR). The SCS and YS are 99 semi-enclosed marginal seas in the NWPO. Seawater in the SCS exhibits oligotrophy characterised by nanomolar levels of N 100 and P (Guo C. et al., 2012), whereas that in the YS exhibits higher trophic statuses (even eutrophication, Liu et al., 2013). 101 The KE exhibits variable trophic statuses, ascribed to the frequent vertical and horizontal mixing of seawater and the 102 combined effects of the Kuroshio and Oyashio currents (Kitajima et al., 2009). The TR is influenced by the Oyashio current, 103 and the concentrations of macronutrients (N and P) in TR seawater can be an order of magnitude higher than those in the KE 104 and SCS (Measures et al., 2006; Isada et al., 2018; Zhang et al., 2020). Considering this variability, the present study aimed 105 to demonstrate (1) the impact of the addition of ship-emitted particles (SEPs) on phytoplankton growth in coastal seas and 106 open oceans of the NWPO, and (2) the contribution of ship emissions to N deposition and the resultant effects on primary

107 production in the NWPO.

108

#### **2. Materials and Methods**

#### 110 2.1. Collection of SEPs

SEP samples were collected by an onboard emission test system from the stack of the heavy-oil-powered vessel *YuKun* during a cruise undertaken on 4–13 November 2015 in the Bohai Sea (Zhang F. et al., 2018 and 2020). Briefly, a sampling pipe was used to direct the ship's emissions from the stack to the particulate sampler. A flue gas analyser was installed in the vessel exhaust pipe to test the concentration of gaseous matter. Before sampling, the flue gas was diluted 1–10 times using a dilution system. The extent of dilution was determined based on the real-time concentration of gaseous matter. Samples were collected on Teflon filters (90 mm diameter) and stored at -20 °C until laboratory analysis and onboard experiments were undertaken.

#### 118 2.2. Experimental design

119 The protocol of the microcosm incubation experiments was designed in accordance with several previous studies (Zhang C. 120 et al., 2018 and 2019a). Briefly, the surface seawater (2-5 m) for the incubation experiment was sampled on the R/V 121 Dongfanghong II during two cruises in 2016 at six stations: M1 and M1B in the KE, E2 in the TR, YS1 in the YS (Cruise I: 122 March-April), and E4 and D5 in the SCS (Cruise II: May-June, Fig. 1). Baseline seawater conditions were determined 123 immediately after sampling, using small volumes of seawater to determine the initial concentrations of Chl a and nutrients (NO<sub>3</sub><sup>-</sup>, NO<sub>2</sub><sup>-</sup>, PO<sub>4</sub><sup>3-</sup> and Si(OH)<sub>4</sub>) at the sampling stations. The remaining sample volumes were screened through a 200 µm 124 125 nylon mesh to remove large zooplankton, and then transferred evenly into acid-washed polycarbonate bottles (Nalgene), 126 which had been rinsed thoroughly with the sampled seawater three times prior to filling. Two types of incubation bottles

were used: bottles with capacities of 20 L for low-SEP additions (0.06–0.14 mg L<sup>-1</sup>) and bottles with capacities of 2 L for 127 128 high-SEP additions (0.59–0.70 mg L<sup>-1</sup>) and various nutrient additions (each in triplicate, Table 1). The SEP loadings in this study were similar to the reportedly cumulative concentrations of atmospheric particles (0.03–0.99 mg L<sup>-1</sup> over a duration of 129 130 1-30 days) in surface seawater (~10 m, Zhang et al., 2019b). Consideration of such a wide range of SEP loadings can help 131 improve our overall understanding of the impact of SEPs on phytoplankton growth. All bottles were incubated in three large 132 vessels where surface irradiance was attenuated by  $\sim 40\%$ , and were maintained at relatively stable temperatures using water 133 pumped continuously from the surface of the ocean. Incubation continued for five/six days for the 20 L bottles and four/five 134 days for the 2 L bottles, with the total incubation time depending on the sample volume. Total (only for 2 L bottles) and 135 size-fractionated (only for 20 L bottles) Chl a were sampled at 07:00-08:00 a.m. each day.

#### 136 2.3. Chemical analysis

In the land-based laboratory, the ultrasonic bath method was used to extract soluble nutrients (i.e. NO<sub>3</sub><sup>-</sup>, NO<sub>2</sub><sup>-</sup>, NH<sub>4</sub><sup>+</sup>, PO<sub>4</sub><sup>3-</sup>, 137 138 and Si(OH)<sub>4</sub>) and trace metals in the SEP samples (Zhang et al., 2019b). The extraction process lasted for 1 hr at 0 °C in 139 deionized water, followed by filtration using 0.45-µm polytetrafluoroethylene syringe filters. The extracting solution of 140 soluble nutrients was determined immediately and that of soluble trace metals needed to be acidified by 1% HNO3 and 141 stored at 4 °C until analysis. In the onboard laboratory, nutrient samples from the baseline seawater (~200 mL) were gently 142 filtered (i.e. vacuum level less than or equal to 0.02 MPa) through acid-washed cellulose acetate filters (Ximengdou, China) into 125 mL polyethylene vials, and stored immediately at -20 °C until laboratory analysis of NO<sub>3</sub><sup>-</sup>+NO<sub>2</sub><sup>-</sup>, PO<sub>4</sub><sup>3-</sup>, and Si(OH)<sub>4</sub> 143 144 was conducted on land. All nutrient samples were analysed via spectrophotometric methods using the SEAL AA3 continuous 145 flow analyser (Grasshoff et al., 1999). Soluble trace metals dissolved from SEP samples were analysed using an inductively 146 coupled plasma mass spectrometer (ICP-MS, Agilent).

# 147 **2.4.** Chl *a* analysis

148 Sampled seawater collected each day from the 2 L incubation bottles was gently (i.e. vacuum level was less than or equal to 149 0.02 MPa) filtered through GF/F filters for total Chl a. For 20 L incubation bottles, sampled seawaters (collected each day) 150 were gently filtered on 20 µm (Millipore), 2 µm (Whatman), and 0.2 µm (Whatman) filters for micro- (>20 µm), nano- (2-20 151  $\mu$ m), and pico- (0.2–2  $\mu$ m) sized Chl *a*, respectively, and total Chl *a* was calculated as the sum of Chl *a* size fractions. The 152 sampled volume of seawater was in the range of 150-300 mL and varied depending on the total Chl a concentration. 153 Immediately after filtering, the samples on the filters were transferred to dark conditions and extracted overnight in 90% 154 acetone at -20 °C (Strickland & Parsons, 1972). Fluorescence was measured directly onboard using a Trilogy fluorometer 155 (Turner Designs).

# 156 2.5. Descriptions of the air emission inventory for shipping and the WRF-CMAQ model

157 Ship emissions were estimated based on the 2015 Automatic Identification System (AIS) data following the methodology described by Fan et al. (2016) and Feng et al. (2019). The coastal/ocean-going ship emission inventories were constructed 158 159 based on all shipping traffic activities and were represented in the model domain as described in Fig. S1. The non-ship 160 emission inventory for the simulation was obtained from the 2015 national emission database (Ding et al., 2019).  $NO_x$ 161 emissions from all anthropogenic sources and shipping traffic in the model domain were 23673 and 1676 kt, respectively. 162 The estimated ship-borne  $NO_x$  emissions in the model domain were within previously reported ranges of  $NO_x$  emissions within 200 nautical miles of the coastline of China. For example, values of 1381, 1443, and 1910 kt were reported by Lv et 163 164 al. (2018), Li et al. (2018), and Fu et al. (2017), respectively. Discrepancies between the reported values can be attributed to (1) increased shipping traffic in 2015 relative to 2013 and differences in the geographical area considered for calculation, and 165 166 (2) differences in AIS data sources and ship register databases.

167

168	The total N deposition fluxes (including oxidised and reduced N) induced by ship emissions were estimated by a combined
169	meteorological-air quality model named the Weather Research and Forecasting (WRF, version 3.3)-Community Multiscale
170	Air Quality (CMAQ, version 4.6) model (Daewon and Kenneth, 2006), and were based on the model results with (base case)
171	and without (no-ship case) airborne ship emissions in 2015. A spatial resolution of $81 \times 81$ km was set up in this study.
172	Additional details about the model setup and evaluation are provided in Text S1, Table S1, and Table S2.

#### 173 **2.6. Data analysis protocol**

Significant differences in the mean Chl *a* concentrations among the various experimental treatments were examined usingone-way analysis of variance (ANOVA).

176

# 177 **3. Results**

#### 178 **3.1.** Baseline surface seawater in the study regions

179 Broadly, the trophic status of baseline seawater increased in the following order: SCS < KE < TR < YS (Table 2). Concentrations of NO<sub>3</sub><sup>-+</sup>NO<sub>2</sub><sup>-</sup> did not exceed 0.10 µmol L<sup>-1</sup> in the SCS and increased to 0.11 µmol L<sup>-1</sup> at M1B and 0.79 µmol 180  $L^{-1}$  at M1 in the KE. These concentrations of NO<sub>3</sub><sup>-+</sup>NO<sub>2</sub><sup>-</sup> reached maximum values of 4.52 µmol L<sup>-1</sup> at E2 in the TR and 181 10.70 µmol L<sup>-1</sup> at YS1 in the YS. A similar pattern was observed for PO<sub>4</sub><sup>3-</sup> and Si(OH)<sub>4</sub> (Table 2). The lowest Chl a 182 concentration ( $\leq 0.14 \ \mu g \ L^{-1}$ ) was also observed in the SCS, with higher values observed in the KE, TR, and YS (0.50–0.92 183 184  $\mu g L^{-1}$ ). Accordingly, we were able to classify the sampling stations into three distinct types based on increasing trophic status (TS), as follows: TSI (oligotrophic status)-A (E4) and TSI-B (D5) in the SCS, TSII (oligo-to-mesotrophic status)-A 185 186 (M1) and TSII-B (M1B) in the KE, and TSIII (meso-to-eutrophic status)-A (E2) in the TR and TSIII-B (YS1) in the YS. This 187 classification can help us better understand phytoplankton responses to SEP addition in seawater characterised by variable 188 trophic statuses and provide a reference for extrapolating our results to other oceanic regions with similar characteristics.

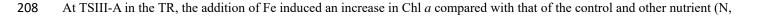
#### 189 3.2. Nutrient limitation in the study regions

190 Seawater in most parts of the SCS is characterised by oligotrophy (Guo C. et al., 2012; Li et al., 2015; Chu et al., 2018), 191 where nutrient concentrations (e.g. N and P) are typically extremely low, which makes it possible for nutrients to co-limit 192 phytoplankton growth (Moore et al., 2013). In this study, the addition of N+P and N+P+Fe induced the most significant 193 increases in Chl a relative to those of the control and single-nutrient treatments (p < 0.05) at TSI-A (days 3–5) and TSI-B 194 (days 4–5, Fig. 2). We found there was no significant difference in Chl a between the N+P and N+P+Fe treatments (p > 0.05), 195 indicating no Fe limitation of phytoplankton. In the single-nutrient treatments, the addition of N at TSI-A, and N or P at 196 TSI-B induced significant differences (p < 0.05) in Chl a relative to that of the control, while the maximum Chl a 197 concentrations were only 24-44% of those in the N+P treatments. Therefore, we conclude that phytoplankton at TSI-A and 198 TSI-B are co-limited by N and P, with N being the primary limiting nutrient.

199

In the KE, both the *Kuroshio* water from the southwest and the *Kuroshio–Oyashio* transition water from the north are characterised by N:P<16, which generally leads to an excess of P relative to N in seawater (Whitney, 2011; Guo X. et al., 2012). In our study, the additions of N, N+P, and N+P+Fe induced the most significant increases in Chl *a* relative to those of the control and P-only treatments (p < 0.05) at TSII-A and TSII-B (days 2–4, Fig. 2). We found no significant difference in Chl *a* in the N, N+P, and N+P+Fe treatments at TSII-A (p > 0.05) and found a significant difference between the N+P/N+P+Fe and N treatments at TSII-B on only one day (day 4). This indicates that phytoplankton were limited primarily by N at both TSII-A and TSII-B.

207



209 P, N+P) treatments (Fig. 2), indicating phytoplankton were likely limited by Fe. This result is consistent with previous

210 studies showing that low availability of Fe is typical of this region (Noiri et al., 2005; Isada et al., 2018). At TSIII-B in the 211 YS, only the N+P+Fe addition experiment was conducted, and we did not find a significant difference relative to the control 212 (p > 0.05, Fig. 2). In addition, Chl a increased noticeably in the control during the incubation experiments, indicating the 213 occurrence of a bloom (Liu et al., 2013). From this, in conjunction with the replete nutrient stocks of the baseline seawater, we infer that phytoplankton at TSIII-B were not limited by N, P, Fe, or their combinations. In the YS, various factors can 214 215 supply replete nutrients to cause annual spring bloom of phytoplankton. These factors include riverine inputs, atmospheric 216 deposition, frequent upwelling of waters due to low water depth (generally <100 m) and strong wind stress, and 217 accumulation of nutrients in winter (Liu et al., 2003; Ren et al., 2011; Liu et al., 2013).

#### 218 **3.3. Response of phytoplankton to SEP addition**

219 The actual concentrations of the SEP components added to the incubated seawater can be calculated by adding the masses of 220 the SEPs per litre of seawater (Table 3). Generally, SEPs provided dissolved inorganic N (DIN, including NO<sub>3</sub><sup>-</sup>, NO<sub>2</sub><sup>-</sup>, and NH<sub>4</sub><sup>+</sup>), various trace metals (especially Fe, Co, Ni, and Zn), and negligible amounts of PO<sub>4</sub><sup>3-</sup> and Si(OH)<sub>4</sub>, according to the 221 222 Redfield ratio and the characteristics of the baseline seawater (Table 2). At TSI-A and TSI-B in the SCS, the addition of low 223 and high SEPs markedly increased the concentrations of DIN (i.e. by 14-243% relative to the baseline seawater, Fig. 3a). 224 Accordingly, the maximum concentrations of Chl a for the low and high SEP treatments at TSI-A were  $\sim$ 1.2- and  $\sim$ 1.5-fold 225 higher than those for the control experiments, respectively (Fig. 3b). Similar phytoplankton responses were also observed at 226 TSI-B. At TSII-A and TSII-B in the KE, the considerable supply of DIN from high-SEP additions increased the maximum 227 Chl a significantly (~1.2- and ~1.4-fold) relative to those of the controls. The contribution of DIN supplied by low-SEP 228 additions was found to be 11% of that of the baseline at TSII-B, and thus the maximum Chl a was found to be only 1.1-fold 229 higher than that of the control (Fig. 3b). At TSII-A, we found no significant difference in Chl a between the control and 230 low-SEP treatments (p < 0.05), which we attribute to the negligible input of DIN by low-SEP additions (Fig. 3). At the TSIII stations, nutrient concentrations were relatively replete, and only the high-SEP additions at TSIII-A induced a significant 231

increase (p < 0.05) in Chl *a* relative to that of the control (Fig. 3b).

#### 233 3.4. Impact of airborne ship emissions on N deposition over the NWPO

234 In general, the total N deposition flux induced by all anthropogenic sources and ship emissions (ship-derived N) showed a 235 similar trend of spatial distribution, i.e. decreasing N deposition flux with increasing distance from the coastline (Fig. 4a and 236 4b). The opposite trend was observed in the relative contribution of ship emissions to the total N deposition flux induced by all anthropogenic sources (Fig. 4c). The ship-induced N deposition flux in the model domain was up to 1.3 g m<sup>-2</sup> yr<sup>-1</sup> (Fig. 237 4b). This is similar to the highest value of 1 g  $m^{-2}$  yr<sup>-1</sup> simulated by Chen et al. (2020). The annual amount of total N 238 239 deposition flux was 1841 kt in 2015. Of this, 1063 kt was associated with air emissions from shipping (~58%). The 240 ship-induced N deposition included the oxidised N deposition of 785 kt formed directly from ship-emitted  $NO_x$  and the 241 indirectly enhanced reduced N deposition of 278 kt due to chemical reactions with ambient NH<sub>3</sub> (Table 4). The indirect 242 shipping-enhanced deposition of reduced N in different seasons accounts for 21-49% of the direct shipping-enhanced 243 deposition of oxidised N (Table 4).

# 244 4. Discussion

### 245 4.1. Fertilisation effects of SEP on phytoplankton growth

On the basis of the phytoplankton response to nutrient and SEP enrichment, we found that the input of N by SEP addition was the primary factor responsible for phytoplankton growth at stations TSI and TSII. This was also supported by the positive correlation between the proportion of N supplied by SEPs relative to N stocks in the baseline seawater (i.e.  $P_{SN} = [N$ supplied by SEP additions/N stocks in the baseline seawater] × 100) and the extent of the phytoplankton response (i.e.  $RC_{Chl}$ a = [Mean in the SEP treatments - Mean in the control]/Mean in the control) × 100, Fig. 5a) in the incubated seawater. Theimportance of N deposition in primary production has been demonstrated in China's coastal seas (Guo C. et al., 2012; Shi etal., 2012) and open oceans of the NWPO (Martino et al., 2014; Zhang et al., 2019b). This is ascribed to increasing 253 anthropogenic N emissions in East Asia (Kim et al., 2014) and primarily N limitation in most regions of the NWPO on the 254 basis of field observations (Duce et al., 2008; Okin et al., 2011), in-situ experiments (Li et al., 2015; Zhang et al., 2019b) and modeling (Dutkiewicz et al., 2012). We note that the slope of the relationship between  $RC_{Chl a}$  and  $P_{SN}$  decreases gradually 255 256 with increasing P<sub>SN</sub>, suggesting that the effects of N nutrients on phytoplankton growth wane with the gradual alleviation of 257 the pressures exerted by N shortage. Although N is the primary limiting nutrient, the stocks of other biologically essential 258 nutrients in incubated seawater also affect phytoplankton growth (Moore et al., 2013; Zhang et al., 2019a). Moreover, a 259 switch in the most deficient nutrient can occur with alteration of the nutrient structure in seawater under the influence of 260 substantial N input (Arrigo, 2005; Zhang C. et al., 2018).

261

262 Although the added amounts of N and/or P in the nutrient treatments were far higher than those in the SEP treatments (Tables 263 1 and 3), the results for these nutrient treatments provide a useful reference to interpret the phytoplankton response to SEP 264 addition at stations TSI and TSII to some extent. In general, the  $RC_{Chla}$  induced by SEP addition was initially similar to that 265 in the nutrient treatments (i.e. N, N+P, and N+P+Fe), and then, with increasing  $P_{SN}$  (as extended from the fitted curve), the 266  $RC_{Chl,a}$  values gradually ranged between those in the N and N+P/N+P+Fe treatments (Fig. 5b). The N supplied by SEP 267 addition in the present study played a key role in stimulating phytoplankton growth owing to the negligible supply of P. This 268 corresponded to similar phytoplankton responses in the N, N+P, and N+P+Fe treatments at TSII-A (P<sub>SN</sub> = 127%, Fig. 5b). 269 With increases in P<sub>SN</sub>, the amount of P added by SEP addition relative to that of the baseline seawater is no longer negligible, 270 and thus, the increases in Chl a associated with the SEP treatments are higher than those associated with the N-only 271 treatment (Fig. 5b). Input of P can promote cell division, which can potentially increase the Chl a concentration by increasing the number of cells (Cavender-Bares et al., 1999; Arrigo, 2005). Meanwhile, when we supposed that 1 µmol L<sup>-1</sup> of 272 N was supplied by SEP addition, the calculated amount of P added (~0.04 µmol L<sup>-1</sup>) was much lower than that in the P-only 273 treatment (0.2 µmol L<sup>-1</sup>). Therefore, the addition of N+P and N+P+Fe induced larger increases in Chl a than the SEP 274

treatments, as observed at TSI-A and TSI-B (Fig. 5b).

276

On the other hand, SEP addition supplied considerable amounts of trace metals such as Zn and/or Fe (Table 3), which have
the potential to facilitate the utilisation of dissolved organic matter as a P source by phytoplankton under P limitation. Such
enhancement of the use of dissolved organic P, induced by atmospheric deposition, has been widely reported in previous
studies (Moore et al., 2013; Browning et al., 2017b; Chu, et al., 2018). Hence, although SEP-derived N was the primary
factor stimulating phytoplankton growth in our study, the impact of P and trace metals may be important when $P_{SN}$ is
sufficiently large, especially in the oligotrophic seawater that constitutes ~60% of the global ocean (Longhurst et al., 1995).
At TSIII-A in the TR, the addition of low and high SEP supplied ~1.6 and ~16 nmol Fe $L^{-1}$ to the incubated seawater,
respectively. However, a significant increase in Chl a was observed only for the high treatments (Fig. 3b). Other trace metals
supplied by SEP addition, such as Zn and Co, might also affect phytoplankton growth in the North Pacific (Table 3,
Crawford et al., 2003; Saito et al., 2008; Jakuba et al., 2012). Because of the experimental conditions, our onboard
incubation experiments did not strictly follow the 'trace metal clean' technique. Accordingly, we could not directly verify the
role of each trace metal in phytoplankton growth. However, it is clear that a considerable input of SEPs can have a
significant fertilisation effect on phytoplankton growth in the TR (Fig. 3b). At TSIII-B in the YS, the negligible difference in
Chl a between the control and SEP treatments is largely due to the baseline nutrient-replete condition that has created an
ideal environment for phytoplankton growth (Fig. 3b, Table 2).

# 293 4.2. Characteristics of ship-induced N deposition

In our study, although ship-borne  $NO_x$  emissions in the model domain account for only 7.1% of the total  $NO_x$  emissions, up to 97% of ship-borne  $NO_x$  could be deposited over the ocean. Hence, the direct contribution of airborne ship emissions to total N deposition could be approximately 43% in this domain (Table 4). Indeed, compared with the rapid decrease in the

297	deposition rates of terrestrial anthropogenic N observed with increasing distance from the East Asian continent (Kim et al.,
298	2014), the sustained emissions associated with shipping play an increasingly important role in N deposition flux over the
299	ocean (Jickells et al., 2017). Moreover, the relative contribution of ship-borne $NO_x$ may increase in the near future, with
300	further NO <sub>x</sub> reductions from power plants and land traffic. Some overestimations are present in the relative contribution of
301	shipping. In particular, this study considered terrestrial NO <sub>x</sub> emissions from only China, excluding other areas of Southeast
302	Asia such as Japan and Korea. However, statistical estimates according to the simulation results suggest that approximately
303	10% of N originating from other terrestrial sources (i.e. excluding China) is deposited over the ocean. Thus, the net effect of
304	overestimation is likely limited.

In addition, we note that shipping traffic indirectly enhanced the deposition of reduced N (Table 4). Previous studies focussed primarily on the contribution of ship-borne NO<sub>x</sub> to N deposition (Jagerbrand et al., 2019; Raudsepp et al., 2019; Zhang J et al., 2019; Chen et al., 2020). However, our study indicates that the impact of ship emissions on reduced N deposition should not be neglected in future studies. This is because the direct emissions of ship-borne NO<sub>x</sub> and SO<sub>2</sub> have the potential to enhance the efficiency of  $NH_4^+$  deposition under saturated  $NH_4^+$  conditions.

### 311 4.3. Impact of ship-induced N deposition on surface Chl a changes over the NWPO

The good nonlinear relationship between  $P_{SN}$  and  $RC_{Chl\,a}$  obtained from the onboard incubation experiments enlightens us to evaluate the general impact of airborne ship emissions on surface Chl *a* changes over the NWPO. Considering the previously published N residence time for coastal waters over one year (Galloway et al., 2003; Boyer and Howarth, 2013), increases in the DIN concentrations in surface seawater induced by ship emissions were estimated using the ship-induced N deposition fluxes (unit: g m<sup>-2</sup> yr<sup>-1</sup>) divided by an annually mixed layer depth (unit: m). The baseline DIN concentration in surface seawater was obtained from the World Ocean Atlas (WOA) 2013 nutrient dataset. Therefore, we could illustrate the spatial distribution of RC<sub>Chl a</sub> over the NWPO on the basis of calculated P<sub>SN</sub>.

320 As shown in Fig. 6, the RC<sub>Chl a</sub> values induced by airborne ship emissions ranged from 1.0% to 7.1% (4.2% on average). The 321 model results for the Baltic Sea also showed that the relative change in phytoplankton productivity (unit: mmol N m<sup>-3</sup>) 322 induced by ship-borne nutrients (dominated by atmospheric N deposition) was no larger than 10% (Raudsepp et al., 2019). 323 Noticeable increases in Chl a concentration were observed in the coastal waters of the YS and open oceans of the NWPO 324 (Fig. 6). This pattern of change is distinct from the spatial distribution of ship-induced N deposition over the ocean (Fig. 4b, Chen et al., 2020), because N stocks in surface seawater also affect the phytoplankton response to external nutrient inputs 325 326 (Noiri et al., 2005; Meng et al., 2016; Zhang et al., 2020). Note that lower RC<sub>Chl a</sub> values were observed in the eastern parts 327 of the ECS, where seawater is characterised by eutrophication due to the influence of the Yangtze diluted water. However, 328 the absolute accumulation of Chl a could be even larger in this region because of the higher stocks of phytoplankton biomass 329 that are present (Meng et al., 2016; Zhang C. et al., 2019a). In addition, atmospheric deposition may have altered the 330 phytoplankton community while having a negligible effect on the Chl a concentration (Meng et al., 2016). 331

332 Our estimates did not include regions for which the N:P ratio in surface seawater exceeded 16:1 (corresponding primarily to 333 nearshore regions), because we considered that phytoplankton were limited primarily by P under these conditions according 334 to the Redfield ratio (Duce et al., 2008; Moore et al., 2013). However, phytoplankton have the ability to trigger 335 acclimatisation mechanisms to cope with P limitation. Such mechanisms include increasing the N:P stoichiometry and 336 utilising dissolved organic phosphorus (Arrigo, 2005; Moore et al., 2013; Zhang et al., 2019a). In addition, ship-induced N 337 deposition likely has a supplementary stimulation impact on phytoplankton, even if N is not the primary limiting nutrient 338 (Zhang et al., 2019a). Hence, the actual area influenced by ship-induced N deposition in the NWPO may not be confined to 339 the N-limiting regions. Further study is needed to encompass the whole ocean and consider areas characterised by variable 340 nutrient-limiting conditions.

# 342 6. Conclusions

343 In this study, we conducted a series of microcosm experiments to elucidate the overall fertilisation effects of SEP addition on phytoplankton growth. By establishing a quantitative relationship between P<sub>SN</sub> and RC<sub>Chl a</sub> on the basis of in-situ microcosm 344 345 experiments, the phytoplankton response to ship-induced N deposition in the NWPO has become predicable to some extent. 346 The WRF-CMAQ model was used to estimate the N deposition flux induced by ship emissions in 2015, and demonstrated the important contribution of ship emissions to the total N deposition flux (~58%) over the NWPO. The  $P_{SN}$  induced by 347 348 airborne ship emissions in the surface seawater of the NWPO was obtained by combining ship-induced N deposition flux 349 from the model results and DIN concentrations from the WOA dataset. Accordingly, we found a noticeable impact of 350 airborne ship emissions on phytoplankton growth indicated by RC<sub>Chl a</sub> in both coastal waters and open oceans of the NWPO. 351 In contrast to open oceans, coastal waters characterised by higher biomasses are more favourable for fixing carbon at the 352 same value of RC<sub>Chl a</sub>. Meanwhile, large phytoplankton with higher sinking rates, generally have higher biomass 353 contributions in coastal waters, and thus are favourable for increasing the export efficiency of fixed carbon due to airborne 354 ship emissions (Maranon, 2015; Zhang C. et al., 2020). Considering the widespread distribution of N-limited regions in the 355 global ocean (Moore et al., 2013) and the rapid spread and deposition of substances emitted in association with worldwide 356 shipping traffic, we posit that the impact of SEPs on marine production may extend to other similar oceanic regions. We 357 foresee an increase in the importance of ship emissions in marine biogeochemical cycles in the near future and suggest that 358 combining multiple measures (including field observations, modeling, and remote sensing) will be necessary to evaluate this 359 impact globally.

### 360 Acknowledgments.

This work was funded by National Natural Science Foundation of China (NSFC) (41876125: Gao; 41906119: Zhang C.; 21677038: Zhang Y.), NSFC and Royal Society travel grant (4141101141: Gao and Shi), NSFC-Shandong Joint Fund (U1906215: Gao), Major State Basic Research Development Program of China (973 Program) (2014CB953701: Gao). Shi is also supported by the Natural Environment Research Council (NE/S00579X/1). We thank the open research cruise NORC2015-05 supported by NSFC Shiptime Sharing Project (project number: 41449905) for supporting the microcosm incubation experiments.

367

## 368 Author contributions

Conceptualization: Chao Zhang, Zongbo Shi, Huiwang Gao; Data curation: Yang Yu, Junri Zhao, Xiaohong, Yao, Xiaohuan
Liu; Formal analysis: Chao Zhang, Zongbo Shi, Yan Zhang; Investigation: Chao Zhang, Yingchun Mu, Junri Zhao, Liming
Feng, Fan Zhang; Methodology: Chao Zhang, Yan Zhang, Huiwang Gao; Resources: Yan Zhang, Junri Zhao, Yingjun Chen,
Jinhui Shi; Visualization: Chao Zhang, Yang Yu; Writing – original draft: Chao Zhang; Writing – review & editing: Zongbo
Shi, Yan Zhang, Xiaohong Yao, Huiwang Gao; Supervision: Zongbo Shi, Yan Zhang, Huiwang Gao; Funding acquisition:
Chao Zhang, Zongbo Shi, Huiwang Gao

375

#### 376 Data and materials availability

377 Relevant data are reported in the text or supplementary material, and data in tables are available on request.

#### 378 References

- Arrigo, K. R., 2005. Marine microorganisms and global nutrient cycles. Nature. 437(7057), 349–355.
  https://doi.org/10.1038/nature04158
- Bencs, L., Horemans, B., Buczynska, A. J., Van G. R., 2017. Uneven distribution of inorganic pollutants in marine air
  originating from ocean-going ships. Environ. Pollut. 222, 226-233. https://doi.org/10.1016/j.envpol.2016.12.052
- Boyd, P. W., Jickells, T., Law, C., Blain, S., Boyle, E., Buesseler, K., Coale, K., Cullen, J., De Baar, H., Follows, M., 2007.
  Mesoscale iron enrichment experiments 1993-2005: Synthesis and future directions. Science. 315(5812), 612-617.
  https://doi.org/10.1126/science.1131669
- Boyer, E. W., Howarth, R. W. (Eds.), 2013. The nitrogen cycle at regional to global scales. Springer Science & Business
  Media.
- Browning, T. J., Achterberg, E. P., Rapp, I., Engel, A., Bertrand, E. M., Tagliabue, A., Moore, C. M., 2017a. Nutrient
  co-limitation at the boundary of an oceanic gyre. Nature. 551(7679), 242. https://doi.org/10.1038/nature24063
- 390 Browning T. J., Achterberg E. P., Yong J. C., Rapp, I., Utermann, C., Engel, A., Moore, C. M., 2017b. Iron limitation of 391 acquisition in the tropical North Atlantic. 15465. microbial phosphorus Nat. Commun. 8(1), 392 https://doi.org/10.1038/ncomms15465
- Cavender-Bares K.K., Mann E.L., Chisholm S.W., Ondrusek M.E., Bidigare R.R., 1999. Differential response of equatorial
   Pacific phytoplankton to iron fertilization. Limnol. Oceanogr. 44(2), 237-246. https://doi.org/10.4319/lo.1999.44.2.0237
- 395 Chen, D., Wang, X., Li, Y., Lang, J., Zhou, Y., Guo, X., Zhao, Y., 2017a. High-spatiotemporal-resolution ship emission 396 inventory of China based AIS data in 2014. Sci. Total Environ. 609, 776-787, on 397 https://doi.org/10.1016/j.scitotenv.2017.07.051
- Chen, D., Wang, X., Nelson, P., Li, Y., Zhao, N., Zhao, Y. H., Lang, J. L., Zhou, Y., Guo, X. R., 2017b. Ship emission inventory and its impact on the PM<sub>2.5</sub> air pollution in Qingdao Port, North China. Atmos. Environ. 166, 351-361.
  https://doi.org/10.1016/j.atmosenv.2017.07.021
- Chen, D., Fu, X., Guo, X., Lang, J., Zhou, Y., Li, Y., Liu, B., Wang, W., 2020. The impact of ship emissions on nitrogen and
  sulfur deposition in China. Sci. Total Environ. 708, 134636. https://doi.org/10.1016/j.scitotenv.2019.134636
- Chien, C. T., Mackey, K. R., Dutkiewicz, S., Mahowald, N. M., Prospero, J. M., Paytan, A., 2016. Effects of African dust
  deposition on phytoplankton in the western tropical Atlantic Ocean off Barbados. Global Biogeochem. Cy. 30(5), 716–734.
  https://doi.org/10.1002/2015GB005334
- Chu, Q., Liu, Y., Shi, J.H., Zhang, C., Gong, X., Yao, X.H., Guo, X.Y., Gao, H.W., 2018. Promotion effect of Asian dust on phytoplankton growth and potential dissolved organic phosphorus utilization in the South China Sea. J. Geophys.
  Res.-Biogeo. 123(3), 1101–1116. https://doi.org/10.1002/2017JG004088
- Corbett, J. J., Fischbeck, P. S., Pandis, S. N., 1999. Global nitrogen and sulfur inventories for oceangoing ships. J. Geophys.
  Res.-Atmos. 104(D3), 3457-3470. https://doi.org/10.1029/1998JD100040
- 411 Crawford, D. W., Lipsen, M. S., Purdie, D. A., Lohan, M. C., Statham, P. J., Whitney, F. A., Putland, J. N., Johnson, W. K.,
- 412 Sutherland, N., Peterson, T. D., Harrison, P. J., Wong, C. S., 2003. Influence of zinc and iron enrichments on phytoplankton
- growth in the northeastern subarctic Pacific. Limnol. Oceanogr. 48(4), 1583-1600, https://doi.org/10.4319/lo.2003.48.4.1583
- 414 Daewon, B., Kenneth, L. S., 2006. Review of the governing equations, computational algorithms, and other components of

- the models-3 community multiscale air quality (cmaq) modeling system. Appl. Mech. Rev. 59(2), 51-77,
  https://doi.org/10.1115/1.2128636
- Djambazov, G., Pericleous, K., 2015. Modelled atmospheric contribution to nitrogen eutrophication in the English Channel
  and the southern North Sea. Atmos. Environ. 102, 191-199. https://doi.org/10.1016/j.atmosenv.2014.11.071
- Ding, D., Xing, J., Wang, S., Liu, K., Hao, J., 2019. Estimated Contributions of Emissions Controls, Meteorological Factors,
   Population Growth, and Changes in Baseline Mortality to Reductions in Ambient PM<sub>2.5</sub> and PM<sub>2.5</sub>-Related Mortality in
   China, 2013 2017. Environ. Health Persp. 127(6), 067009. https://doi.org/10.1289/EHP4157
- 422 Duce, R. A., La Roche, J., Altieri, K., Arrigo, K. R., Baker, A. R., Capone, D. G., Cornell, S., Dentener, F., Galloway, J.,
- 423 Ganeshram, R. S., Geider, R. J., Jickells, T., Kuypers, M. M., Langlois, R., Liss, P. S., Liu, S. M., Middleburg, J. J., Moore,
- 424 C. M., Nickovic, S., Oschlies, A., Pedersen, T., Prospero, J., Schlitzer, R., Seitzinger, S., Sorensen, L. L., Uematsu, M., Ulloa,
- 425 O., Voss, M., Ward, B., Zamora, L., 2008. Impacts of atmospheric anthropogenic nitrogen on the open ocean. Science.
  426 320(5878), 893–897. https://doi.org/10.1126/science.1150369
- Dutkiewicz, S., Ward, B. A., Monteiro, F., Follows, M. J., 2012. Interconnection of nitrogen fixers and iron in the Pacific
  Ocean: Theory and numerical simulations. Global Biogeochem. Cy. 26(1). https://doi.org/10.1029/2011GB004039
- Eyring, V., Isaksen, I. S., Berntsen, T., Collins, W. J., Corbett, J. J., Endresen, O., Grainger, R. G., Moldanova, J., Schlager, H.
  Stevenson, D., 2010. Transport impacts on atmosphere and climate: Shipping. Atmos. Environ. 44(37), 4735-4771.
  https://doi.org/10.1016/j.atmosenv.2009.04.059
- Fan, Q., Zhang, Y., Ma, W., Ma, H., Feng, J., Yu, Q., Yang X., Simon, K., Chen, L., 2016. Spatial and seasonal dynamics of
  ship emissions over the Yangtze River Delta and East China Sea and their potential environmental influence. Environ. Sci.
  Technol. 50(3), 1322-1329. https://doi.org/10.1021/acs.est.5b03965
- Feng, J., Zhang, Y., Li, S., Mao, J., Patton, A. P., Zhou, Y., Ma, W., Liu, C., Kan, H., Huang, C., An, J., Li, L., Shen, Y., Fu,
  Q., Wang, X., Liu, J., Wang, S., Ding. D., Chen, J., Ge, W., Zhu., H., Walker, K., 2019. The influence of spatiality on
  shipping emissions, air quality and potential human exposure in the Yangtze River Delta/Shanghai, China. Atmos. Chem.
  Phys. 19(9), 6167-6183. https://doi.org/10.5194/acp-19-6167-2019
- Fu M, Liu H, Jin X, He K., 2017. National-to port-level inventories of shipping emissions in China. Environ. Res. Lett.
  12(11), 114024. https://doi.org/10.1088/1748-9326/aa897a
- Galloway, J. N., Aber, J. D., Erisman, J. W., Seitzinger, S. P., Howarth, R. W., Cowling, E. B., Cosby, B. J., 2003. The
  nitrogen cascade. Bioscience. 53(4), 341-356. https://doi.org/10.1641/0006-3568(2003)053
- 443 Grasshoff, K., Kremling, K., & Ehrhardt, M., 1999. Methods of seawater analysis, 3 edn., Wiley-VCH.
- Guo, C., Yu, J., Ho, T.-Y., Wang, L., Song, S., Kong, L., Liu, H., 2012. Dynamics of phytoplankton community structure in
  the South China Sea in response to the East Asian aerosol input. Biogeosciences. 9(4), 1519-1536.
  https://doi.org/10.5194/bg-9-1519-2012
- Guo, X., Zhu, X., Wu, Q., Huang, D., 2012. The Kuroshio nutrient stream and its temporal variation in the East China Sea. J.
  Geophys. Res.-Oceans. 117, C01026. https://doi.org/10.1029/2011JC007292
- Hassellov, I. M., Turner, D. R., Lauer, A., Corbett, J. J., 2013. Shipping contributes to ocean acidification. Geophys. Res.
  Lett. 40(11), 2731-2736. https://doi.org/10.1002/grl.50521
- 451 Hunter, K. A., Liss, P. S., Surapipith, V., Dentener, F., Duce, R., Kanakidou, M., Kubilay, N., Mahowald, N., Okin, G., Sarin,
- 452 M., Uematsu, M., Zhu, T., 2011. Impacts of anthropogenic SO<sub>x</sub>, NO<sub>x</sub> and NH<sub>3</sub> on acidification of coastal waters and shipping

- 453 lanes. Geophys. Res. Lett. 38(13). https://doi.org/10.1029/2011GL047720
- 454 IPCC., 2007. Climate change 2007: impacts, adaptation and vulnerability. Contribution of Working Group II to the Fourth
- 455 Assessment Report of the Intergovernmental Panel on Climate Change. In: Parry, M.L., Canziani, O.F., Palutikof, J.P., van
- 456 der Linden, P.J., Hanson, C.E. (Eds.). Cambridge University Press, Cambridge, UK, p. 976
- 457 Isada, T., Hattori-Saito, A., Saito, H., Kondo, Y., Nishioka, J., Kuma, K., Hattori, H., McKay, R.M.L., Suzuki, K., 2018.
- 458 Responses of phytoplankton assemblages to iron availability and mixing water masses during the spring bloom in the
  459 Oyashio region, NW Pacific. Limnol. Oceanogr. 64(1), 197-216. https://doi.org/10.1002/lno.11031
- 460 Ito, A., Shi, Z. B., 2016. Delivery of anthropogenic bioavailable iron from mineral dust and combustion aerosols to the ocean.
  461 Atmos. Chem. Phys. 16(1), 85-99. https://doi.org/10.5194/acp-16-85-2016
- 462 Ito, A., 2013. Global modeling study of potentially bioavailable iron input from shipboard aerosol sources to the ocean.
  463 Global Biogeochem. Cy. 27(1), 1-10. https://doi.org/10.1029/2012GB004378
- Jagerbrand, A. K., Brutemark, A., Sveden, J. B., Gren, I., 2019. A review on the environmental impacts of shipping on
  aquatic and nearshore ecosystems. Sci. Total Environ. 695, 133637. https://doi.org/10.1016/j.scitotenv.2019.133637
- 466 Jakuba, R. W., Saito, M. A., Moffett, J. W., Xu, Y., 2012. Dissolved zinc in the subarctic North Pacific and Bering Sea: its 467 speciation, producers. Global Biogeochem. distribution. and importance to primary Cy. 26(2). 468 https://doi.org/10.1029/2010GB004004
- Jickells, T., An, Z., Andersen, K. K., Baker, A., Bergametti, G., Brooks, N., Cao, J., Boyd, P., Duce, R., Hunter, K., 2005.
  Global iron connections between desert dust, ocean biogeochemistry, and climate. Science. 308(5718), 67-71.
  https://doi.org/10.1126/science.1105959
- Jickells, T. D., Buitenhuis, E., Altieri, K., Baker, A. R., Capone, D., Duce, R. A., Dentener, F., Fennel, K., Kanakidou, M.,
  LaRoche, J., Lee, K., Liss, P., Middelburg, J. J., Moore, J. K., Okin, G., Oschlies, A., Sarin, M., Seitzinger, S., Sharples, J.,
  Singh, A., Suntharalingam, P., Uematsu, M., & Zamora, L. M., 2017. A reevaluation of the magnitude and impacts of
  anthropogenic atmospheric nitrogen inputs on the ocean. Global Biogeochem. Cy. 31(2), 289–305.
  https://doi.org/10.1002/2016GB005586
- Kitajima, S., Furuya, K., Hashihama, F., Takeda, S., Kanda, J., 2009. Latitudinal distribution of diazotrophs and their
  nitrogen fixation in the tropical and subtropical western North Pacific. Limnol. Oceanogr. 54, 537-547.
  https://doi.org/10.4319/lo.2009.54.2.0537
- Kim, I.-N., Lee, K., Gruber, N., Karl, D. M., Bullister, J. L., Yang, S., Kim, T.-W., 2014. Increasing anthropogenic nitrogen in the North Pacific Ocean. Science. 346(6213), 1102-1106. https://doi.org/10.1126/science.1258396
- Liu H., Fu M., Jin X., Shang Y., Shindell D., Faluvegi G., Shindell C., He K., 2016. Health and climate impacts of
  ocean-going vessels in East Asia. Nat. Clim. Change. 6(11), 1037–1041. https://doi.org/10.1038/nclimate3083
- Liu, S., Zhang, J., Chen, S. Z., Chen, H., Hong, G., Wei, H., Wu, Q., 2003. Inventory of nutrient compounds in the Yellow
  Sea. Cont. Shelf Res. 23(11), 1161-1174. https://doi.org/10.1016/S0278-4343(03)00089-X
- Liu, Y., Zhang, T., Shi, J., Gao, H., Yao, X., 2013. Responses of chlorophyll a to added nutrients, Asian dust, and rainwater in
  an oligotrophic zone of the Yellow Sea: Implications for promotion and inhibition effects in an incubation experiment. J.
  Geophys. Res.-Biogeo. 118(4), 1763-1772. https://doi.org/10.1002/2013JG002329
- Li C, Borken-Kleefeld J, Zheng J, Yuan Z, Ou J, Li Y, Wang, Y., Xu, Y., 2018. Decadal evolution of ship emissions in China
  from 2004 to 2013 by using an integrated AIS-based approach and projection to 2040. Atmos. Chem. Phys. 18(8), 6075-6093.

- 491 https://doi.org/10.5194/acp-18-6075-2018
- 492 Li, Q., Legendre, L., Jiao, N., 2015. Phytoplankton responses to nitrogen and iron limitation in the tropical and subtropical
- 493 Pacific Ocean. J. Plankton Res. 37(2), 306–319. https://doi.org/10.1093/plankt/fbv008

Longhurst, A., Sathyendranath, S., Platt, T., Caverhill, C., 1995. An estimate of global primary production in the ocean from
 satellite radiometer data. J. Plankton Res. 17(6), 1245–1271. https://doi.org/10.1093/plankt/17.6.1245

Lv Z, Liu H, Ying Q, Fu M, Meng Z, Wang Y, Wei., W., Gong. H., He, K., 2018. Impacts of shipping emissions on PM2.5
pollution in China. Atmos. Chem. Phys. 18(21), 15811-15824. https://doi.org/10.5194/acp-18-15811-2018

- Maranon, E., 2015. Cell size as a key determinant of phytoplankton metabolism and community structure. Annu. Rev. Mar.
  Sci. https://doi.org/10.1146/annurev-marine-010814-015955
- Martino, M., Hamilton, D., Baker, A. R., Jickells, T. D., Bromley, T., Nojiri, Y., Quack, B., Boyd, P. W., 2014. Western
  Pacific atmospheric nutrient deposition fluxes, their impact on surface ocean productivity. Global Biogeochem. Cy. 28(7),
  712-728. https://doi.org/10.1002/2013GB004794
- Measures, C., Cutter, G., Landing, W., Powell, R., 2006. Hydrographic observations during the 2002 IOC Contaminant
  Baseline Survey in the western Pacific Ocean. Geochem. Geophy. Geosy. 7, Q03M06. https://doi.org/
  10.1029/2004GC000855
- Meng, X., Chen, Y., Wang, B., Ma, Q., Wang, F., 2016. Responses of phytoplankton community to the input of different aerosols in the East China Sea. Geophys. Res. Lett. 43(13), 7081-7088. https://doi.org/10.1002/2016GL069068
- Moore, C., Mills, M., Arrigo, K., Berman-Frank, I., Bopp, L., Boyd, P., Galbraith, E., Geider, R. J., Guieu, C., Jaccard, S.,
  2013. Processes and patterns of oceanic nutrient limitation. Nat. Geosci. 6(9), 701-710. https://doi.org/10.1038/NGEO1765
- Noiri, Y., Kudo, I., Kiyosawa, H., Nishioka, J., Tsuda, A., 2005. Influence of iron and temperature on growth, nutrient
  utilization ratios and phytoplankton species composition in the western subarctic Pacific Ocean during the SEEDS
  experiment. Prog. Oceanogr. 64(2), 149-166. https://doi.org/10.1016/j.pocean.2005.02.006
- Okin, G. S., Baker, A. R., Tegen, I., Mahowald, N. M., Dentener, F. J., Duce, R. A., Galloway, J. N., Hunter, K., Kanakidou,
  M., Kubilay, N., Prospero, J. M., Sarin, M., Surapipith, V., Uematsu, M., Zhu, T., 2011. Impacts of atmospheric nutrient
  deposition on marine productivity: Roles of nitrogen, phosphorus, and iron. Global Biogeochem. Cy. 25(2).
  https://doi.org/10.1029/2010GB003858
- Raudsepp, U., Maljutenko, I., Kõuts, M., Granhag, L., Wilewska-Bien, M., Hassellöv, I. M., Eriksson, K. M., Johansson. L.,
  Jalkanen. J. P., Karl M., Matthias. V., Moldanova. J., 2019. Shipborne nutrient dynamics and impact on the eutrophication in
  the Baltic Sea. Sci. Total Environ. 671, 189-207. https://doi.org/10.1016/j.scitotenv.2019.03.264
- Ren, J. L., Zhang, G. L., Zhang, J., Shi, J. H., Liu, S. M., Li, F. M., Jin, J., Liu, C. G., 2011. Distribution of dissolved aluminum in the southern Yellow Sea: Influences of a dust storm and the spring bloom. Mar. Chem. 125(1), 69–81. https://doi.org/10.1016/j.marchem.2011.02.004
- Saito, M.A., Goepfert, T.J., Ritt, J.T., 2008. Some thoughts on the concept of colimitation: three definitions and the
  importance of bioavailability. Limnol. Oceanogr. 53(1), 276–290. https://doi.org/10.2307/40006168
- Schroth, A. W., Crusius, J., Sholkovitz, E. R., Bostick, B. C., 2009. Iron solubility driven by speciation in dust sources to the
  ocean. Nat. Geosci. 2(5), 337-340. https://doi.org/10.1038/ngeo501
- Shi, J., Gao, H., Zhang, J., Tan, S., Ren, J., Liu, C., Liu, Y., Yao, X., 2012. Examination of causative link between a spring
  bloom and dry/wet deposition of Asian dust in the Yellow Sea, China. J. Geophys. Res.-Atmos. 117, D17304.

- 529 https://doi.org/10.1029/2012JD017983
- 530 Strickland, J. D. H., Parsons, T. R., 1972. A practical handbook of seawater analysis.
- 531 Turner, D. R., Edman, M., Gallego-Urrea, J. A., Claremar, B., Hassellov, I. M., Omstedt, A., Rutgersson, A., 2017. The potential 532 future contribution acidification of the Baltic Sea. of shipping to Ambio. 1-11. https://doi.org/10.1007/s13280-017-0950-6 533
- 534 UNCTAD. Review of maritime transport 2019. New York. October 2019. https://unctad.org/en/
  535 PublicationsLibrary/rmt2019\_en.pdf.
- Whitney, F. A., 2011. Nutrient variability in the mixed layer of the subarctic Pacific Ocean, 1987–2010. J. Oceanogr. 67(4),
  481-492. https://doi.org/10.1007/s10872-011-0051-2
- Yau, P. S., Lee, S. C., Corbett, J. J., Wang, C., Cheng, Y., Ho, K. F., 2012. Estimation of exhaust emission from ocean-going
  vessels in Hong Kong. Sci. Total Environ. 431, 299-306. https://doi.org/10.1016/j.scitotenv.2012.03.092
- Zhang, C., Gao H. W., Yao, X. H., Shi, Z. B., Shi, J. H, Yu, Y., Meng, L., Guo, X. Y., 2018. Phytoplankton growth response
  to Asian dust addition in the northwest Pacific Ocean versus the Yellow Sea. Biogeosciences, 15(3), 749-765.
  https://doi.org/10.5194/bg-15-749-2018
- Zhang, C., Yao, X. H., Chen, Y., Chu, Q., Yu, Y., Shi, J. H., Gao, H. W., 2019a. Variations in the phytoplankton community
  due to dust additions in eutrophication, LNLC and HNLC oceanic zones. Sci. Total Environ. 669, 282-293.
  https://doi.org/10.1016/j.scitotenv.2019.02.068
- Zhang, C., Ito, A., Shi, Z. B., Aita, M. N., Yao, X. H., Chu, Q., Shi, J. H., Gong, X., Gao, H.W., 2019b. Fertilization of the
  Northwest Pacific Ocean by East Asia air pollutants. Global Biogeochem. Cy. 33(6), 690-702.
  https://doi.org/10.1029/2018GB006146
- Zhang, C., He, J. Y., Yao, X. H., Mu, Y., C., Guo, X. Y., Ding, X. K., Yu, Y., Shi, J., H., Gao, H.W., 2020. Dynamics of
  phytoplankton and nutrient uptake following dust additions in the northwest Pacific. Sci. Total Environ. 739, 139999.
  https://doi.org/10.1016/j.scitotenv.2020.139999
- Zhang, F., Chen, Y., Tian, C., Lou, D., Li, J., Zhang, G., Matthias, V., 2020. Emission factors for gaseous and particulate
  pollutants from offshore diesel engine vessels in China. Atmos. Chem. Phys. 16(10), 6319-6334.
  https://doi.org/10.5194/acp-16-6319-2016
- Zhang, F., Chen, Y., Chen, Q., Feng, Y., Shang, Y., Yang, Gao, H., Tian, C., Li, J., Zhang, Gan., Matthias, V., Xie, Z., 2018.
  Real-World Emission Factors of Gaseous and Particulate Pollutants from Marine Fishing Boats and Their Total Emissions in China. Environ. Sci. Technol. 52(8), 4910-4919. https://doi.org/10.1021/acs.est.7b04002
- Zhang, J., Gao, Y., Leung, L. R., Luo, K., Liu, H., Lamarque, Fan, J., Yao X., Gao H., Nagashima, T., 2019. Impacts of
  climate change and emissions on atmospheric oxidized nitrogen deposition over East Asia. Atmos. Chem. Phys. 19(2),
  887-900. https://doi.org/10.5194/acp-19-887-2019
- Zhang Y., Yang X., Brown R., Yang L., Morawska L., Ristovski Z., Fu Q., Huang C., 2017. Shipping emissions and their
  impacts on air quality in China. Sci. Total Environ. 581, 186-198. https://doi.org/10.1016/j.scitotenv.2016.12.098

# 564 List of Figures and Tables

565 Figure 1. Locations of the sampling stations where the onboard microcosm experiments were performed. The base map 566 reflects water depths of the ocean.

Figure 2. Responses of Chl *a* concentrations to various nutrient additions over the duration of the incubation experiments.
"Control", "N", "P", "Fe", "N+P", and "N+P+Fe" in this figure indicate the control, N, P, Fe, N+P, and N+P+Fe treatments, respectively.

**Figure 3.** (a) Proportion of N supplied by ship-emitted particles (SEPs) relative to N stocks in the baseline seawater ( $P_{SN}=[N]$  supplied by SEP additions/N stocks in the baseline seawater]×100) for low and high SEP treatments at the sampling stations. (b) Responses of total Chl *a* to low and high SEP additions during the incubation experiments. "Control-20 L" and "Control-2 L" indicate the control treatments for 20 L and 2 L incubation bottles, respectively. "Low" and "High" indicate low-SEP treatments and high-SEP treatments, respectively.

Figure 4. Annual N (including oxidised N and reduced N) deposition fluxes in the northwest Pacific Ocean from (a) all
anthropogenic sources, (b) ship emissions, and (c) contributions of ship emissions to the annual N deposition fluxes.

**Figure 5.** Relationships between relative change in Chl *a* (RC<sub>Chl *a*</sub>, ([Mean in the ship emitted particle (SEP) treatments-Mean in the control]/Mean in the control)×100) and proportion of N supplied by SEPs relative to N stocks in the baseline seawater ( $P_{SN}$ , [N supplied by SEP additions/N stocks in the baseline seawater]×100) for (a) SEP and (b) nutrient (N, N+P, and N+P+Fe) treatments. The olive open symbols in Fig. (a) were obtained from SEP treatments at TSIII-A (E2, Fe limitation) and TSIII-B (YS1, no limitation of N, P, Fe), which were not used to fit the curve. In (b), the dashed panel region corresponds to the fitted curve in (a), and the line out of the dashed panel was extended from the fitted curve (a). The  $P_{SN}$  (x-axis) in (b) corresponds, in increasing order, to stations TSII-A (M1), TSII-B (M1B), TSI-B (D5), and TSI-A (E4).

**Figure 6.** Relative change in Chl *a* ( $RC_{Chl a}$ ) in surface seawater owing to ship-induced N deposition.  $RC_{Chl a}$  was based on the empirical equation obtained from the incubation experiments as shown in Fig. 5a. The results in this figure were obtained by excluding the area where N:P ratios in the surface seawater exceeded 16:1 according to the World Ocean Atlas 2013 nutrient dataset.

588

- **Table 1.** Treatments applied to the microcosm incubation experiment.
- **590 Table 2.** Baseline conditions at the sampling stations.
- 591 Table 3. Amounts of macro- and micro-nutrients (soluble trace metals) added for the low and high SEP treatments.
- **Table 4.** Seasonal and annual N deposition fluxes induced by ship emissions and all anthropogenic sources (kt N yr<sup>-1</sup>).
- 593